PHASE IDENTIFICATION AND SATURATION DETERMINATION IN CARBON DIOXIDE FLOODING OF WATER FLOODED CHALK USING X-RAY COMPUTED TOMOGRAPHY

Ben Niu, Wei Yan, Alexander A. Shapiro, Erling H. Stenby
Department of Chemical and Biochemical Engineering, Technical University of Denmark

This paper was prepared for presentation at the International Symposium of the Society of Core Analysts held in Noordwijk, The Netherlands 27-30 September, 2009

ABSTRACT

As an effective method to cope with green-house gas emission, and to enhance oil recovery, injection of carbon dioxide (CO_2) into water flooded petroleum reservoirs has obtained increasing attention. In the laboratory studies, identification of different phases and determination of their saturations by use of X-ray computed tomography (CT) is the key problem to visualize flow and to get insight into the mechanisms of CO_2 injection. The flooding process is essentially three-phase, and involves interaction between oil, water and CO_2 (mutual solubility, change of acidity, swelling of the oil, etc.). The purpose of our study is to investigate experimentally the possibility and potential problems of identifying different phases and quantifying their saturations during CO_2 flooding. Laboratory experiments on injection of CO_2 into chalk cores from the Danish North Sea, saturated with Isopar-L petroleum mixture and distilled water, with various combinations of dopants, have been carried out under the pressures varying in the low to medium range. The experiments utilized CT imaging to visualize the in-situ saturations of the fluids. An optimization method was suggested for the image data analysis, in order to correct the out-of-range data due to low energy level scanning and inhomogeneity of chalk. During experiments, strong adsorption of some dopant on the chalk cores was observed. Sensitivity of chalk to different dopants is discussed. Based on recorded data during CO_2 flooding, as well as on the image data and production profiles of the different phases, the detailed data analysis was conducted. The key factors for the successful application of the X-ray computed tomography to the multiphase flows in a chalk rock were identified. The necessary conditions for successful experiments are suggested.

INTRODUCTION

The carbon dioxide injection into petroleum reservoirs has been considered for enhanced oil recovery (EOR) since early 1950's. Attention to this process is currently growing due to the global warming. This process is characterized by complex phase behavior and interaction between different phases: oil, water and CO_2. The mechanisms of multiphase flow and thermodynamic properties of various phases have been well established and discussed by many researchers, both theoretically [1] and experimentally [2]. In realistic conditions, displacement is affected by presence of the three phases (water, oil, and carbon dioxide) and chemical interaction between rock and the fluids. Identification of all three phases and their distribution in reservoir rock by the

application of X-ray computer tomography (CT) may provide useful practical information for understanding the process of CO_2 injection.

X-ray CT has been applied to core analysis in the oil industry over thirty years [3]. It has also been applied to recovery studies, sample characterization, formation damage, etc. [4]. For example, Zitha et al. [5] and Du et al. [6] recently investigated CO_2 rheology in porous media. Izgec et al. [7] studied the chemical reactions associated with injection and storage of CO2 in carbonate formations. Jikich et al. [8] measured the sorption isotherms of CO_2 in coal cores. It should be noted that most of the recent studies deal with two-phase processes. A few papers on three phase identification either do not illustrate in-situ saturation measurements or conduct the experiments at low pressure condition to keep gas as low density vapor phase, which cannot represent reservoir conditions. Vinegar et al. [9] discussed the mechanisms of X-ray CT scanner, properties of the dopants, and three phase flow study, but without detailed analysis of the three phase in-situ saturations. Chatzis et al. [10] applied X-ray CT to study the physical properties of porous media and saturation profiles during two- and three-phase flow in gravity-assisted displacement processes, with qualitatively visualizations of three phase fluid distributions. Lackner et al. [11] investigated X-ray energy levels for three-phase saturation measurements and conducted three phase experiments under low pressure, without analysis of phase saturations. There are few discussions on the three phase measurements in the chalk core with CO_2 flooding.

In our study, four chalk cores from the Danish North Sea are used as material. Key factors on the successful application of X-ray CT on the identification of three-phase flows under CO_2 flooding are discussed based on the experimental data obtained.

EXPERIMENT

Equipment

The CT scanner used in our study is a fourth generation Siemens SOMATOM scanner (figure 1) with 1200 stationary detectors. The X-ray tube rotates around the object in a 360° circular path. As the beam passes through the object, the lower energy photons are preferentially absorbed. The attenuation coefficient is usually scaled and reported as a CT number. CT numbers are generally presented in terms of an internationally standardized number scale subdivided into Hounsfield units (HU). The scale is linear, with CT numbers for air and water defined as –1000 and 0 respectively. The CT scanner has three different energy levels: 80kV, 120kV, and 137kV, and a higher energy level provides better resolution. The maximum CT number is 3071 at all energy levels. An individual CT scan produces a digital 2-D image map of the X-ray attenuation in a tomographic slice through the object, and the image information is stored in a 512 by 512 matrix. The lighter color on the image indicates higher CT numbers. A series of 2-D images can be used to construct a 3-D image. All image analysis were performed by special graphical softwares FPImage (http://www.fpimage.com) and ImageJ (http://rsbweb.nih.gov/ij/).

Two kinds of X-ray core holders were used in the experiments: an aluminum core holder with a maximum operation pressure of 100 bar, and a carbon fiber wrapped core holder with a maximum operation pressure of 1000 bar and a maximum temperature of 150 ^{o}C. The schematic of experimental setup is shown in figure 2.

Experimental Procedure

Four similar core flooding experiments at room temperature and different pressures were carried out to investigate if different phases could be identified simultaneously. Table 1 provides an overview of all the experiments. A light mineral oil, Isopar-L and n-decane were used as oil phase individually in the different experiments. Two kinds of dopant were selected for distilled water. One was potassium iodide (KI), which is widely used in core analysis with X-ray CT scanner. The other was sodium tungstate dihydrate ($Na_2WO_4 \cdot 2H_2O$), which had been applied in the previous experiments with chalk cores [12].

Table 2 shows the properties of fluids used in this work without dopant. CO_2 is a liquid at 65 bar and 100 bar. The density of CO_2 approaches to that of n-decane and Isopar-L as pressure increases. This indicates that at least two phases are required to be doped to obtain substantial CT number difference between different phases under high pressure.

To identify the in-situ saturations, dual energy levels, 80 kV and 120 kV, were chosen, with composite factors (mA·s), 250 mA·s and 330 mA·s respectively. These two composite factors are the largest values which can be chosen in each energy level to reduce the beam hardening effects. At 137kV, the CT scanner can not perform continuous scanning for more than 20 images due to the high temperature of the tube, although the image quality can be improved a little compared with that at 120 kV. Our choice of the energy levels was based on the image quality as well as the tube life of X-ray CT scanner.

The core holder was installed horizontally on the CT platform. In order to guarantee accurate image positioning, the CT core holder was fixed during the flooding and only moved for scanning between different floodings. The injection rate was 0.1 cc/min. The CT images were taken every two mm along a core. All four experiments share a similar general procedure:

1. Scan dry core, CO_2 saturated core, doped oil saturated core, and doped water saturated core with dual energy. If necessary, clean the core with toluene and ethanol before changing the saturating fluid;
2. Flood the core with doped oil until S_{wi} is reached;
3. Flood the core with doped water until S_{or} is reached;
4. Flood the core with CO_2 until no fluid is produced;
5. Clean and dry the core.

A dual energy scan was taken at the end of each step. Comparison between the scanning data of the dry core before and after the experiment is important for error estimation. During the flooding produced oil, water and gas were separated at atmospheric condition and their volumes were recorded.

Saturation Determination

Saturation determination based on the measured CT numbers has been well established, for two phases,

$$CT_w S_w + CT_o S_o = CT_{wo} \quad (1)$$

$$S_w + S_o = 1 \tag{2}$$

with solution

$$S_o = \frac{CT_{wo} - CT_w}{CT_o - CT_w} \tag{3}$$

For three phases, the corresponding system of equations is

$$CT_{w1}S_w + CT_{o1}S_o + CT_{g1}S_g = CT_{wog1} \tag{4}$$
$$CT_{w2}S_w + CT_{o2}S_o + CT_{g2}S_g = CT_{wog2} \tag{5}$$
$$S_w + S_o + S_g = 1 \tag{6}$$

with solution

$$S_o = \frac{(CT_{wog1} - CT_{w1})(CT_{g2} - CT_{w2}) - (CT_{wog2} - CT_{w2})(CT_{g1} - CT_{w1})}{(CT_{o1} - CT_{w1})(CT_{g2} - CT_{w2}) - (CT_{o2} - CT_{w2})(CT_{g1} - CT_{w1})} \tag{7}$$

$$S_g = \frac{(CT_{wog1} - CT_{w1})(CT_{o2} - CT_{w2}) - (CT_{wog2} - CT_{w2})(CT_{o1} - CT_{w1})}{(CT_{o2} - CT_{w2})(CT_{g1} - CT_{w1}) - (CT_{o1} - CT_{w1})(CT_{g2} - CT_{w2})} \tag{8}$$

In eqs. 1 to 8, the phase saturations S_i are expressed in terms of the measured CT numbers CT_i of various fluid saturated cores. Subscripts o, w and g represent oil, water, and gas respectively. Their combinations, wo and wog suggest the existence of various phases in the core. Subscripts 1 and 2 indicate the two different energy levels, 80 kV and 120 kV in our experiments respectively.

The dependence of a calculated saturation on CT numbers can be evaluated in two ways. One way is to differentiate eqs. 3 and 7 with respect to each of the CT numbers. For example, for two phases

$$\frac{\delta S_o}{\delta CT_o} = \frac{CT_w - CT_{wo}}{(CT_o - CT_w)^2} \tag{9}$$

For three phases,

$$\frac{\delta S_o}{\delta CT_{o1}} = \frac{\left[(CT_{wog1} - CT_{w1}) \cdot (CT_{g2} - CT_{w2}) - (CT_{wog2} - CT_{w2}) \cdot (CT_{g1} - CT_{w1})\right](CT_{w2} - CT_{g2})}{\left[(CT_{o1} - CT_{w1}) \cdot (CT_{g2} - CT_{w2}) - (CT_{o2} - CT_{w2}) \cdot (CT_{g1} - CT_{w1})\right]^2} \tag{10}$$

The other way is to evaluate the coefficient matrix. Equations 1-2 and 4-6 are linear equations, and expressed in the general form,

$$\mathbf{Ax} = \mathbf{B} \tag{11}$$

For two phases,

$$\mathbf{A}_2 = \begin{bmatrix} 1 & \dfrac{CT_o}{CT_w} \\ 1 & 1 \end{bmatrix},\ \mathbf{x}_2 = \begin{bmatrix} S_w \\ S_o \end{bmatrix},\ \text{and}\ \mathbf{B}_2 = \begin{bmatrix} \dfrac{CT_{wo}}{CT_w} \\ 1 \end{bmatrix}$$

For three phases, by substituting eq. 6 into eq. 4 and 5 to eliminate S_w, one obtains

$$\mathbf{A}_3 = \begin{bmatrix} a_{11} & a_{12} \\ a_{21} & a_{22} \end{bmatrix} = \begin{bmatrix} 1 & \dfrac{CT_{o1} - CT_{w1}}{CT_{g1} - CT_{w1}} \\ 1 & \dfrac{CT_{o2} - CT_{w2}}{CT_{g2} - CT_{w2}} \end{bmatrix},\ \mathbf{x}_3 = \begin{bmatrix} S_g \\ S_o \end{bmatrix}\ \text{and}\ \mathbf{B}_3 = \begin{bmatrix} \dfrac{CT_{wog1} - CT_{w1}}{CT_{g1} - CT_{w1}} \\ \dfrac{CT_{wog2} - CT_{w2}}{CT_{g2} - CT_{w2}} \end{bmatrix}$$

The determinant or the conditional number of coefficient matrix $\mathbf{A}_2$ and $\mathbf{A}_3$ indicate whether eq. 11 is well- or ill-conditioned.

RESULTS AND DISCUSSION

Experiment 1

In the first experiment, selection of dopants was in accordance with the study in [12]. Figure 3 shows the CT number in the plug from position 2 mm to 40 mm (the CT numbers at the very ends of the plug are omitted due to the noise created by the aluminum filter). Since the penetrating power of X-rays through the material increases with the potential difference across the tube, the CT number at 80kV is always higher than that at 120 kV from the fluids used in our experiments. It should be noted that at both energy levels, the CT numbers for different fluids are non-distinguishable around the inlet, and approach the upper limit of the CT scanner, 3071. The phase saturations calculated by eqs. 7 and 8 are shown in figure 4. The average gas saturation, 64.4%, was close to the value, 61%, calculated from mass balance. But the average water and oil saturations were not in a reasonable range, exhibiting even negative values.

As shown in the CT and 3-D reconstruction images (figure 5), the CT numbers at the inlet of the dry core after the experiment are much higher than those before the experiment (figure 3) and almost reach the upper limit of the CT scanner. This indicates that strong adsorption of the dopant happens during the experiment, which spoils its results.

Experiment 2

To avoid adsorption, lower $Na_2WO_4 \cdot H_2O$ concentrations at 1 and 3 wt% were tried. Figure 6 shows the CT numbers of the plug saturated with different fluid. The CT numbers of Isopar-L and CO_2 are close to each other with an average difference of around 9. An implication of this observation is that the three-phase flooding can be treated as a pseudo two phase flooding in CT visualization, with the doped water as one phase and CO_2/Isopar-L as another. Figure 6 also indicates that water doped with 1 wt% $Na_2WO_4 \cdot H_2O$ can not provide enough contrast in CT number and 3 wt% $Na_2WO_4 \cdot H_2O$ was finally used. However, adsorption in the chalk was observed again and it was concluded that $Na_2WO_4 \cdot H_2O$ was not adequate to our chalk samples.

Experiment 3

In this experiment, Isopar-L was deliberately not doped to take advantage of its similar CT numbers to the high pressure CO_2 at 65 bar and 15 ^oC. Since Isopar-L and CO_2 can be treated as one pseudo phase in CT visualization, only the water saturation was measured here and the other two saturations were not determined. Step 3 in the general procedure was deliberately skipped in this experiment to investigate if CO_2 can mobilize the irreducible water.

The difference of CT numbers between CO_2 and Isopar-L induces at maximum ± 0.003 error in the CO_2/Isopar-L saturations calculated by eq. 9. Figure 7 shows fluid saturations calculated by using CT numbers at 120 kV, whose average value is in a good agreement with those calculated from mass balance. Compared with the water saturation before CO_2 flooding, the water saturation at the end of the core has increased by around 0.03. Meanwhile, no water production was observed during the CO_2 flooding. It seems that the water mobilized by the injected CO_2 is captured at the end of the core by capillary pressure.

Figure 8 shows the distribution of pixel CT numbers in the region of interest on the CT image (The region of interest excludes bright circle area, which is characteristic of high CT number and induced by the beam hardening effect.). Both software FPImage and ImageJ provide similar results. The histograms from experiments 1, 2 and 3 indicate that the CT number distribution is very close to normal distribution, which is usual for a homogeneous sample. However, some deviations occur at the areas of heterogeneity (figure 9). Both the 3-D image and 2-D image at 120 kV indicate that core 3 contains high-density non-porous inclusions, which do not contribute to the flow and should be excluded for calculating the average values.

As indicated in figures 3 and 6, by using dopant, a decent contrast in CT numbers for different fluids is obtained at 120 kV. However, at 80 kV, there is a danger that some CT numbers will be beyond the upper limit of the CT scanner, as illustrated in figure 9. ImageJ does not account for that effect and thus provide erroneous average CT numbers.

To obtain correct CT numbers, an optimization method, the nonlinear Huber estimation [13], was used to fit the CT numbers on an image. Compared with the Levenberg-Marquardt method, this method has the advantage of confining wild points in fitted data and faster convergence. Figure 9 also shows the application of the nonlinear Huber estimation. The differences between the average CT numbers from ImageJ and from our method are 25 and 96 for two cases respectively. Figure 10 compares the water saturation determined using data at 80 kV and 120 kV. It can be seen that if the 80 kV data were not corrected using our method, a significant deviation could be resulted. Therefore, re-estimation of the average CT number using the nonlinear Huber estimation is necessary when there are a lot of data points beyond the upper limit of the CT scanner.

Experiment 4

In this experiment, the back pressure was increased to 100 bar where full miscibility can be achieved. The flooding procedure simulates CO_2 injection into a water flooded reservoir as described in the general experimental procedure.

Data from position 0 mm to 28 mm was plotted and analyzed (Table 3) for illustration. For the results at 80 kV, to account for pixels with CT numbers higher than the upper limit of the CT scanner, the Huber estimation was used to get the correct average CT numbers.

In Table 3, the calculated saturations are clearly unsatisfactory since some values are out of the range [0, 1]. The large error can be explained by the determinant of matrix **A** in eq. 11. The system of equations is well-conditioned if the determinant is far from zero. This can be easily achieved in two-phase scanning where CT_o is much smaller than CT_w. Furthermore, the scanning is often performed at the high energy level, 120 kV, where the CT number can be more accurately measured and the upper limit of the CT scanner is not a problem. For three-phase scanning, however, the determinant becomes far from zero if a_{12} and a_{22} are largely different from each other. Although CT_{i1} and CT_{i2} (i=o, w, g) are strongly different at two energy levels, the differences between a_{12} and a_{22} are not that large, especially for liquefied CO_2. As shown in table 3, det($\mathbf{A}_3$) approaches to zero, which indicates that eq. 11 is ill-conditioned. In addition, the CT numbers obtained at 80 kV have larger errors compared to those at 120 kV due to the upper limit of the CT scanner as explained in Experiment 3 and the poorer image quality at lower energy scanning. This further affects the determination of three-phase saturations

By differentiating eq. 7 with respect to CT_{w1}, CT_{o1}, and CT_{g1}, similar to eq. 10, the sensitivity of S_o to the individual CT numbers can be calculated (table 3). It is clear that S_o is most sensitive to the change of CT_{o1}, e.g., if $\delta CT_{o1} = 1$, the maximum absolute change on the S_o can be as large as 0.127. The error estimation reveals the reasons for inaccurate three-phase saturations.

Vinegar and Wellington suggested selecting a K_{edge} dopant for determining three-phase saturations [8]. CT scanning just above the K_{edge} energy will see a sudden increase in the attenuation coefficient. Therefore, if two dopants are used and one of the dopants has K_{edge} between the two scanning energy levels, it is possible to make (CT_o-CT_w), or a_{12} and a_{22}, have opposite signs at two energy levels. And if the absolute values of a_{12} and a_{22} are not too close to zero, $\mathbf{A}_3$ will become well-conditioned In the possible dopants with K_{edge} between our energy levels 120 kV and 80 kV [8], most of them are compounds containing heavy elements, such as lead nitrate ($Pb(NO_3)_2$) and thallium fluoride (TlF). Those dopants are rarely in use in core analysis perhaps due to toxicity. And one also should be aware of the potential adsorption problem if a new dopant is used.

CONCLUSION

Important conclusions from these experiments are:

1. Since $Na_2WO_4 \cdot 2H_2O$ tends to be adsorbed in our chalk samples, even at low concentration, KI was finally selected to dope the water phase. Comparison of the dry core images before and after experiment is important to reveal the adsorption problem.
2. High pressure three-phase flooding can be visualized as pseudo two-phase flooding, where the gas and oil phases have similar CT numbers and are treated as one phase. This provides an alternative for future three-phase experiments, where the most interested phase can be identified under a single energy level.

3. CT number in a homogeneous chalk sample shows normal distribution at both energy levels 80 kV and 120 kV. The nonlinear Huber estimation has proved to be an useful tool to obtain the correct average CT number at 80 kV, where a non-negligible portion of CT numbers are beyond the upper limit of the CT scanner.
4. The CT numbers of the iodododecane doped oil phase, the KI doped water phase, and the high density CO_2 phase increase similarly when the energy level changes from 120 to 80 kV, which makes eq. 11 ill-conditioned and calculated saturations sensitive to smaller errors in CT numbers. This is the major reason for us to give up the simultaneous determination of the three-phase saturations in the current study.
5. To make eq. 11 well-conditioned, one possible way is to use a dopant with K_{edge} between two energy levels.

ACKNOWLEDGEMENT

This study is carried out under the project "Enhanced Oil Recovery through CO_2 Utilization" funded by the Danish National Advanced Technology Foundation.

REFERENCES

1. Zick A.A., "A Combined Condensing/Vaporizing Mechanism in the Displacement of Oil by Enriched Gases", Paper SPE 15493 presented at the SPE Annual Technical Conference and Exhibition, New Orleans, Louisiana, 5-8 October 1986.
2. E. A. Turek, R.S. Metcalfe, R.E. Fishback, "Phase Behavior of Several CO_2/West-Texas-Reservoir-Oil Systems", *SPE Reservoir Engineering*, (1988)**3**, 2, p. 505-516.
3. A. Kantzas., "Investigate of Physical Properties of Porous Rocks and Fluid Flow Phenomena in Porous Media using Computer Assisted Tomography", *In Situ*, (1990)**14**, 1, p. 77-132.
4. Withjack E.M., C. Devier, and G. Michael., "The Role of X-Ray Computed Tomography in Core Analysis", Paper SPE 83467 presented at the SPE Western Regional/AAPG Pacific Section Joint Meeting, Long Beach, California, 19-24 May 2003.
5. Zitha P.L.J., Q.P. Nguyen, and P.K. Currie., "Effect of Flow Velocity and Rock Layering on Foam Flow: an X-ray Computed Tomography Study", Paper SPE 80530 presented at the SPE Asia Pacific Oil and Gas Conference and Exhibition, Jakarta, Indonesia, 9-11 September 2003.
6. Du D.X., P.L.J. Zitha, and M.G.H. Uijttenhout, "Carbon Dioxide Foam Rheology in Porous Media: A CT Scan Study", *SPE Journal*, (2007)**12**, 2, p. 245-252.
7. Izgec O., B. Demiral, H. Bertin, and S. Akin, "CO_2 Injection in Carbonates", Paper SPE 93773 presented at the SPE Western Regional Meeting, Irvine, California, 30 March-01 April 2005.
8. Jikich S.A., R. McLendon, K. Seshadri, G. Irdi and D.H. Smith, "Carbon Dioxide Transport and Sorption Behavior in Confined Coal Cores for Carbon Sequestration", *SPE Reservoir Evaluation & Engineering*, (2009)**12**, 1, p.124-136.
9. Vinegar H.J. and S.L.Wellington, "Tomographic Imaging of Three-Phase Flow experiment". *Rev.Sci.Instrum.*, (1987)**58**, 1, p. 96-107.
10. Chatzis I., A. Kantzas, F.A.L. Dullien, "On the Investigation of Gravity-Assisted Inert Gas Injection Using Micromodels, Long Berea Sandstone Cores, and Computer-Assisted Tomography" Paper 18284 presented at the SPE Annual Technical Conference and Exhibition, Houston, Texas, 2-5 October 1988.

11. Lackner A.S., G. Haaskjold, and O. Torsaeter, "Selecting X-Ray Energy Levels for Three-Phase Saturation Measurements", Paper SPE 95098 presented at the SPE Latin American and Caribbean Petroleum Engineering Conference, Rio de Janeiro, Brazil, 20-23 June 2005.
12. S.Y. Yu. I. Akervoll, O. Torsaeter, J.A. Stensen, J. Kleppe and S.H. Midtlyng, "History Matching Gas Injection Processes with In-Situ Saturation Measurements and Process Hysteresis", Paper SPE 48842 presented at the SPE International Conference and Exhibition in China held in Beijing, China, 2-6 November, 1998.
13. Madsen K. and H.B. Nielsen, "Finite Algorithm for Robust Linear Regression", *BIT Numerical Mathematics*, (1993)**30,** p. 682-699.

Table 1. Overview of core flooding experiments

Plug sample properties					P and T		Fluids and dopant		
Name	Length (mm)	Diameter (mm)	Porosity (%)	k_{water} (md)	P (bar)	T (^oC)	Oil and dopant (wt %)	Water and dopant (wt%)	Gas
Core#1	44.00	25.69	35.50	0.32	65	15	Isopar-L 5% Iodododecane	Distilled water 7% $Na_2WO_4 \cdot H_2O$	CO_2
Core#2	77.02	25.72	40.00	0.13	65	15	Isopar-L without dopant	Distilled water 1 % $Na_2WO_4 \cdot H_2O$ 3 % $Na_2WO_4 \cdot H_2O$	CO_2
Core#3	37.93	25.82	25.74	0.16	65	15	Isopar-L without dopant	Distilled water 5 wt% KI	CO_2
Core#4	74.82	37.04	26.74	0.23	100	15	n-decane, 5% Iodododecane	Distilled water 3 wt% KI	CO_2

Table 2. Fluid properties at laboratory temperature 15^{o}C

	Isopar-L		n-Decane		Water		CO_2	
Pressure (bar)	Density (g/ml)	Viscosity (cp)	Density (g/ml)	Viscosity (cp)	Density (g/ml)	Viscosity (cp)	Density (g/ml)	Viscosity (cp)
Atm	0.779	1.290	0.734	0.987	0.999	1.001	1.80E-3	0.015
65	-	-	0.739	1.065	1.002	0.998	0.848	0.080
100	-	-	0.742	1.108	1.004	0.996	0.890	0.089

Table 3. Three phase saturation and error estimation for experiment 4

Position (mm)	So	Sg	det(A_3)	$\frac{\delta S_o}{\delta CT_{w1}}$	$\frac{\delta S_o}{\delta CT_{o1}}$	$\frac{\delta S_o}{\delta CT_{g1}}$
0	-1.171	1.412	0.027	-0.043	0.011	-0.102
4	0.929	0.092	0.100	0.011	-0.115	0.004
8	0.121	0.573	0.088	-0.001	-0.052	-0.008
12	0.326	0.428	0.054	0.009	-0.096	0.010
16	0.073	0.496	0.120	-0.012	-0.038	-0.009
20	0.044	0.486	0.084	-0.007	-0.037	-0.002
24	0.897	-0.022	0.087	-0.001	-0.058	0.009
28	-1.046	1.117	0.018	0.008	-0.127	0.032

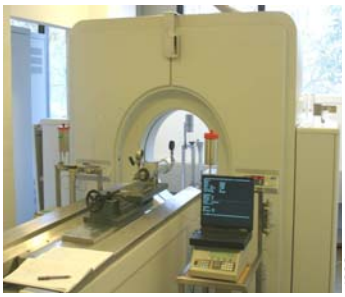

Figure 1. X-ray CT Scanner

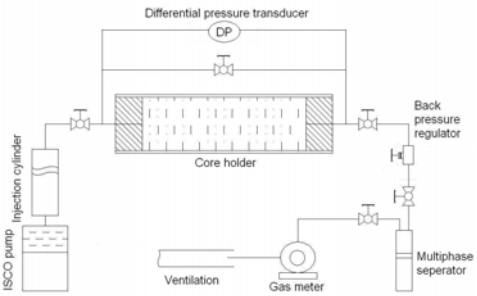

Figure 2. Schematic of experimental setup

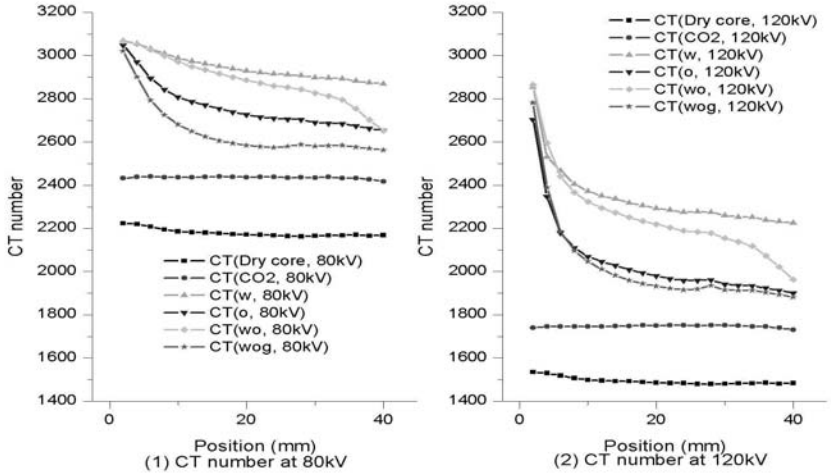

Figure 3. CT number at different energy levels (Experiment 1): (1) 80kV (2) 120kV

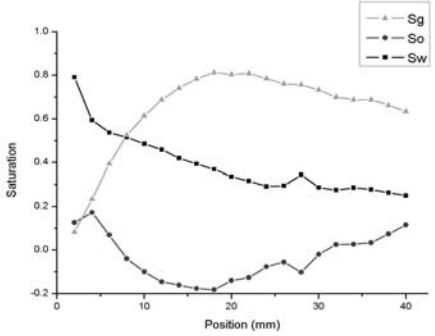

Figure 4. Three phase saturation (Experiment 1)

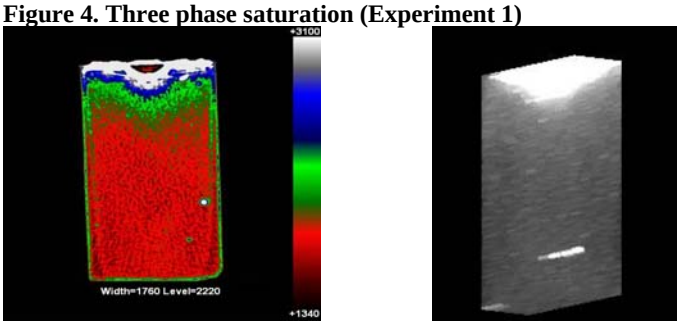

Figure 5. CT and 3-D reconstruction images (120 kV) of a dry core after the experiment

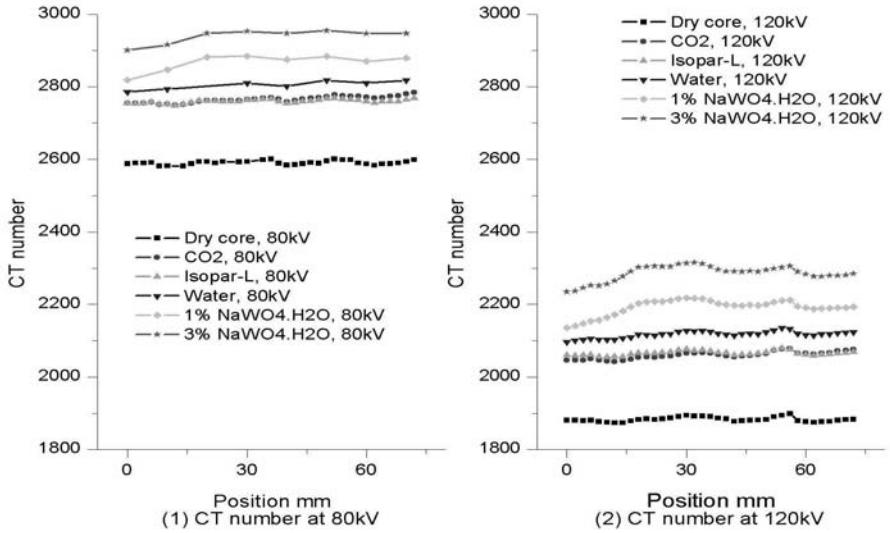

Figure 6. CT number at different energy levels (Experiment 2): (1) 80kV (2) 120kV

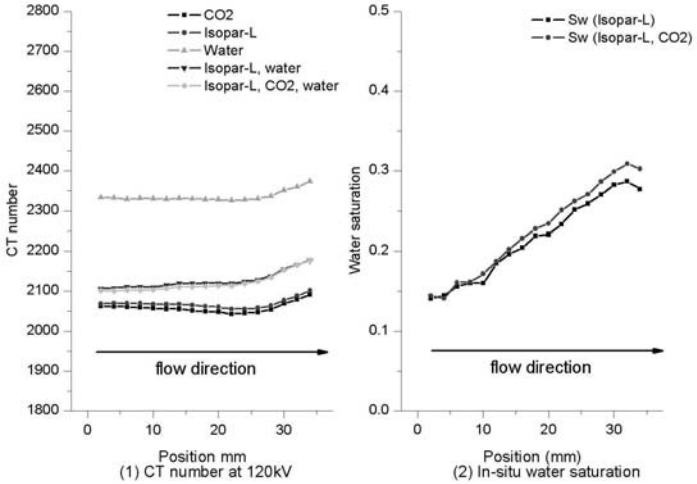

Figure 7. Results from Experiment 3: (1) CT number at 120kV (2) In-situ Saturation

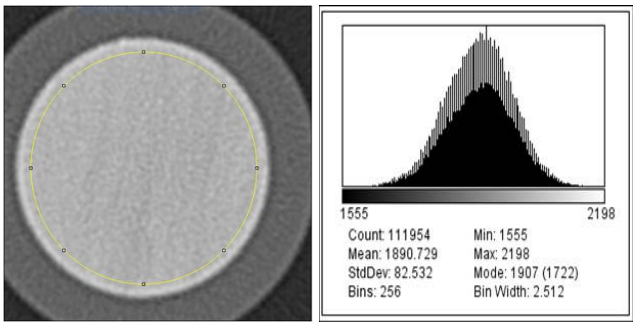

Figure 8. CT number distribution in the region of interest

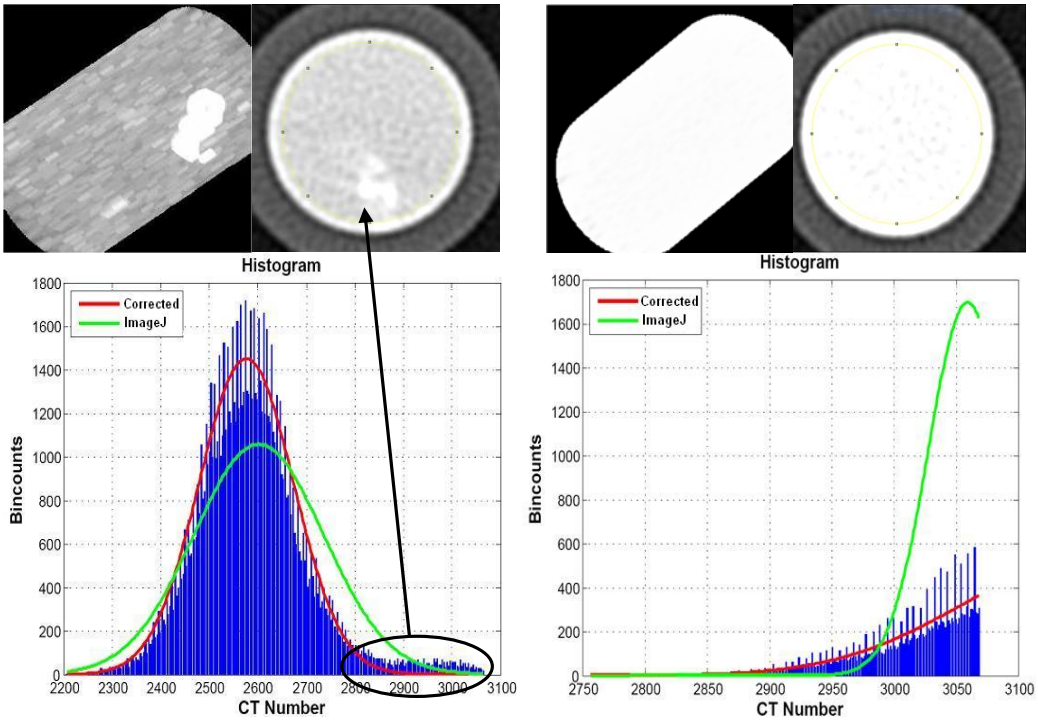

Figure 9. Limitation of ImageJ: (1) inhomogeneity of the core (2) upper limit of CT scanner

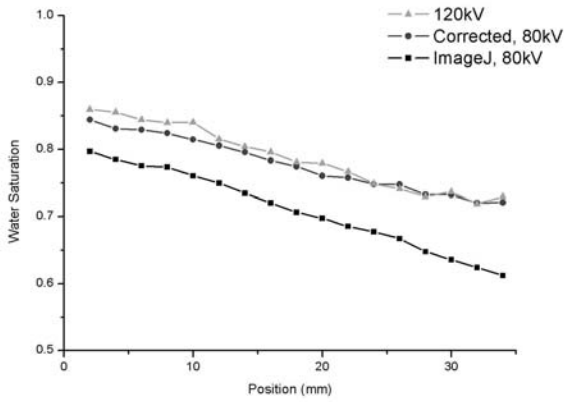

Figure 10. Comparison of water saturation (Experiment 3)